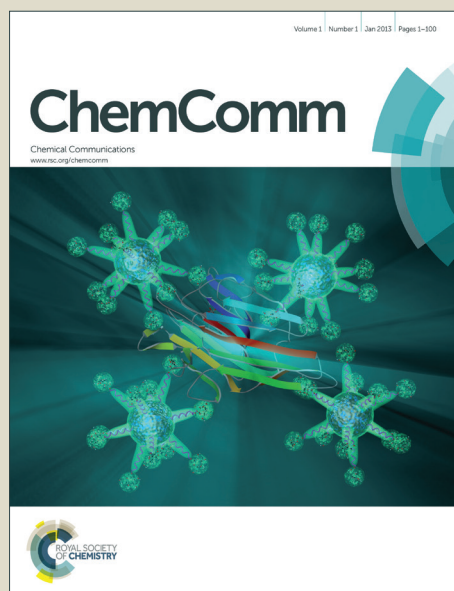


ChemComm

Accepted Manuscript



This is an *Accepted Manuscript*, which has been through the Royal Society of Chemistry peer review process and has been accepted for publication.

Accepted Manuscripts are published online shortly after acceptance, before technical editing, formatting and proof reading. Using this free service, authors can make their results available to the community, in citable form, before we publish the edited article. We will replace this *Accepted Manuscript* with the edited and formatted *Advance Article* as soon as it is available.

You can find more information about *Accepted Manuscripts* in the [Information for Authors](#).

Please note that technical editing may introduce minor changes to the text and/or graphics, which may alter content. The journal's standard [Terms & Conditions](#) and the [Ethical guidelines](#) still apply. In no event shall the Royal Society of Chemistry be held responsible for any errors or omissions in this *Accepted Manuscript* or any consequences arising from the use of any information it contains.

Cite this: DOI: 10.1039/c0xx00000x

www.rsc.org/xxxxxx

COMMUNICATION

Structural Effect on the Resistive Switching Behavior of Triphenylamine-Based Poly(azomethine)s

Wenbin Zhang,^{a,b,§} Cheng Wang,^{c,§} Gang Liu,^{a,†} Jun Wang,^b Yu Chen^{c,†} and Run-Wei Li^{a,†}

Received (in XXX, XXX) Xth XXXXXXXXXX 20XX, Accepted Xth XXXXXXXXXX 20XX

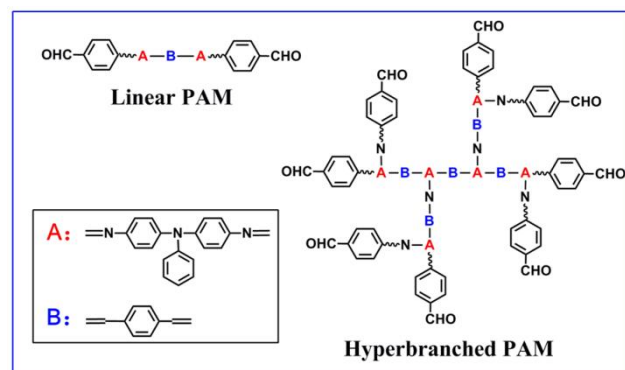
DOI: 10.1039/b000000x

Linear and hyperbranched poly(azomethine)s (PAMs) based on triphenylamine moieties are synthesized and used as the functioning layers in the Ta/PAM/Pt resistive switching memory devices. Comparably, the hyperbranched PAM with isotropic architecture and semi-crystalline nature shows enhanced memory behaviors with more uniform distribution of the HRS and LRS resistances.

By providing inexpensive, lightweight, optically transparent and CMOS compatible modules on mechanically flexible plastic substrates, polymer memories have demonstrated great potential as information storage components in nowadays consumer digital gadgets.¹ Rather than encoding '0' and '1' as the amount of charges stored in a silicon cell, resistive switching memory stores data in an different matter, for instance, based on the high and low resistance states (HRS and LRS) of a metal/insulator/metal structure in response to the external electric field.²

Various polymers, including conjugated polymers, polymers with pendent chromophores, and donor-acceptor polymers, have been demonstrated with memory switching characteristics.³ Similar to the other organic electronic devices, most of the polymers used in memories are linear in structure. In contrast to the linear counterparts, hyperbranched polymers exhibit unique three dimensional structures, good solubility, low melting temperature and solution viscosity, and excellent physiochemical properties.⁴ More importantly, the charge carrier transport, which was found to be anisotropic and strongly depend on the orientation and packing mode of the molecules, can be efficiently enhanced in the isotropic architecture of the hyperbranched polymers.⁵ With its propeller like geometry with a dihedral angle of around 120° between the phenyl rings connected to the central nitrogen atom, triphenylamine (TPA) molecule is considered as an interesting building block to construct hyperbranched conjugated polymers for electronic applications

Aromatic poly(azomethine)s (PAMs) are a class of materials composed of azomethine (C=N) unities and benzene rings alternatively in the backbone, and possessing the merits of easy molecular design and synthesis, good thermal stability, excellent mechanical strength, ability to form metal chelates, liquid crystalline properties and non-linear optical properties.⁶ In this work, conjugated linear and hyperbranched PAMs with triphenylamine chromophores in the polymer backbone have been synthesized *via* comparatively convenient one step condensation polymerization of aldehydes and amines (see Scheme 1, S1 and ESI† for the detail synthesis and characterization), and the structural effect on their memory switching behaviors have been comparably investigated.



Scheme 1 Molecular structures of the linear and hyperbranched PAMs.

The building blocks of the linear and hyperbranched PAMs are chemically identical, except for the spatial arrangement of the triphenylamine chromophores. The structures of the as-synthesized PAMs were confirmed by ¹H nuclear magnetic resonance (¹H NMR) and Fourier transform infrared (FTIR). The ¹H NMR signals with the chemical shifts of 8.1-7.9 ppm (linear PAM) and 8.2-7.9 ppm (hyperbranched PAM) correspond to the proton resonance of the C=N groups in respective PAMs. The signals at 7.4-7.0 ppm are ascribed to the protons on the aromatic rings of the triphenylamine moieties.⁷ In the FTIR spectra, the absorption peaks at 1618 cm⁻¹ and 1583 cm⁻¹ are ascribed to the formation of C=N groups (Fig. S1 of ESI†).^{7b} Due to the presence of triphenylamine chromophores in the main chains, both the linear and hyperbranched PAMs show good solubilities in common polar organic solvents of tetrahydrofuran, methylene chloride, chloroform, *N*-methyl pyrrolidone and dimethyl formamide.^{7b} The number-average molecular weight (*M_n*) of the linear and hyperbranched PAMs are 5.1×10³ and 3.6×10³, respectively. GPC traces of the two PAMs are shown in Fig. S2 of ESI.† In comparison to that of the linear PAM, the GPC trace of the hyperbranched PAM is narrower, which implies its more uniform molecular weight distribution. The UV-Visible absorption spectra of the PAMs, which show absorption bands of the π-π* transition of the conjugated backbone at the shorter wavelength region and the coupling between the n-π* and π-π* transitions of the arylamine moieties at the longer wavelength region, respectively, are displayed in Fig S3.† Both PAMs exhibit excellent thermal stability with the onset decomposition (10% weight loss) temperatures of 470 °C and 458 °C, respectively (Fig. S4). The onset oxidation potentials for the linear and hyperbranched PAMs are 0.86 V and 0.90 V, leading to the HOMO/LUMO energy levels of -5.28 eV/-2.85 eV and -5.32 eV/-2.93 eV, respectively (Fig. S5 of ESI†).

X-ray diffraction (XRD) techniques have been used to check the crystallinity of the two PAMs (**Fig. 1**). In good agreement with the reported literatures, linear PAM is amorphous with broad diffractive peaks in the 2θ range of 5° - 90° .⁵ In obvious contrast, the hyperbranched PAM is semi-crystalline with diffractive peaks at $2\theta = 20^\circ$, 24° , and 30° , respectively. Transmission electron microscopic (TEM) images of the linear and hyperbranched PAMs are also shown in **Fig. 1c** and **1d**, respectively. Apparently, the linear PAM is non-crystalline while the hyperbranched counterpart shows localized crystalline regions.⁸ We also investigate the topographies of the PAM films by atomic force microscopy (AFM) technique in a tapping mode before depositing top electrodes. **Fig. 1e** and **1f** show $2\ \mu\text{m} \times 2\ \mu\text{m}$ AFM images of the linear and hyperbranched PAMs, respectively. The linear PAM clearly shows uneven morphology of a rod-like structure, which is probably arising from the irregular agglomeration of the polymer chains into wool-balls.⁹ On the other hand, the hyperbranched PAM, which possesses relatively less polymer chains folding with larger steric hindrance, displays a uniform nanofilm. Meanwhile, the surface root-mean-square roughness of the hyperbranched PAM film is smaller ($0.76\ \text{nm}$) than that of the linear PAM film ($1.23\ \text{nm}$).

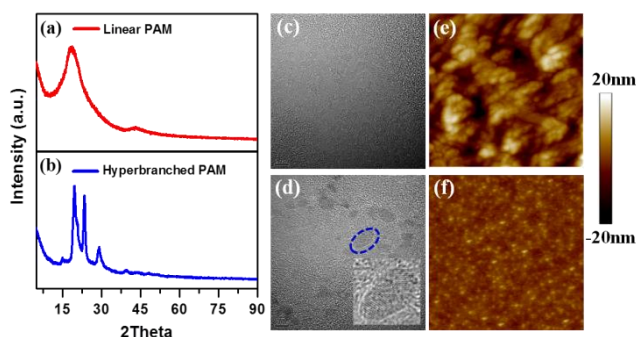


Fig. 1 X-ray diffractive patterns of the (a) linear and (b) hyperbranched PAMs powders. TEM and AFM images of the (c,e) linear and (d,f) hyperbranched PAM films, respectively.

The resistive switching performances of the two PAMs are demonstrated by the current-voltage characteristics of the Ta/PAM/Pt structured devices (**Fig. 2**). A compliance current of 10^{-3} has been preset to avoid device breakdown from overstriking. It is found that the forming operations are always necessary for both polymer devices to be set to the LRS for the first time (**Fig. S6** of ESI[†]). Afterwards, a negative voltage of $-0.41\ \text{V}$ can reset the linear PAM device to the HRS, while a subsequent positive sweep of $1.40\ \text{V}$ can set the linear PAM device to the LRS again (**Fig. 2a**). The HRS to LRS transition can be defined as the “set” or “write” process, and accordingly the LRS to HRS transition is defined as the “reset” or “erase” process. Both the HRS and LRS can be read nondestructively and are stable after removing the power supply, thus completing the “forming-read-erasing-rewriting” cycles of a nonvolatile memory with a ON/OFF ratio over 10^2 . The linear PAM device behaves similarly after being left in air for three month, except for a notable change in the device resistance and the switching voltages. In comparison, the hyperbranched PAM can be set and reset with the sweeping voltages of $1.73\ \text{V}$ and $-0.53\ \text{V}$, respectively, and its resistive switching behavior can be reproduced with good accuracy after three months (**Fig. 2b**).

The endurance performance of the Ta/PAM/Pt was also evaluated in ambient atmosphere by cyclic switching operations. **Fig. 2c** and **2d** show the evolution of the linear and hyperbranched PAM device resistances in the first 128 cycles,

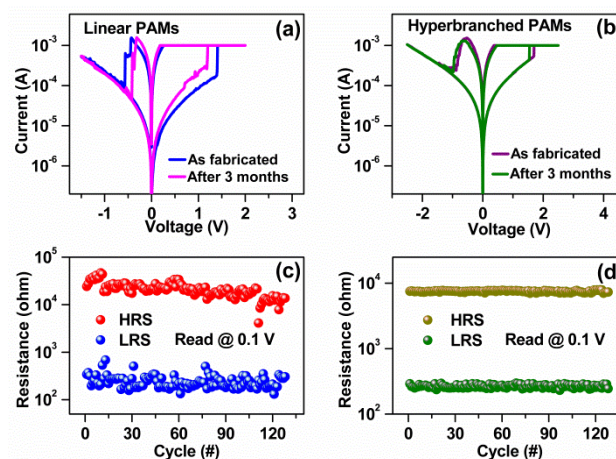


Fig. 2 The current-voltage switching and endurance performance of the Ta/PAM/Pt memory devices fabricated with the (a,c) linear and (b,d) hyperbranched PAMs, respectively.

respectively. The resistance values in each DC sweep were read at $0.1\ \text{V}$. For the Ta/linear PAM/Pt stacks, the LRS resistance decreases rapidly while the HRS resistance fluctuates in less than one order of magnitude. For the Ta/hyperbranched PAM/Pt memory devices, much more uniform distribution of the HRS and LRS resistances are observed. We also count the resistance values of HRS and LRS in all the switching cycles. As expected, a narrow distribution of R_{HRS} ($7.5 \pm 0.2\ \text{k}\Omega$) and R_{LRS} ($270 \pm 15\ \Omega$) are obtained in the Ta/hyperbranched PAM/Pt memory, while the resistance values of Ta/linear PAM/Pt exhibit relatively fluctuated distribution range of $21 \pm 7\ \text{k}\Omega$ (R_{HRS}) and $250 \pm 80\ \Omega$ (R_{LRS}). We have also used Weibull analysis to further quantify the uniformity of the PAM devices (details can be found in ESI[†]). Generally, larger Weibull exponent (k) and smaller standard deviation (Δ) to mean (μ) ratio (Δ/μ) correspond to superior uniformity of the parameters under evaluation.¹⁰ For the Pt/linear PAM/Ta stack, the Δ/μ values of the HRS and LRS resistances are 0.3200 and 0.3333 , respectively. By contrast, the HRS and LRS resistances of the hyperbranched PAM device feature smaller Δ/μ values of 0.0267 and 0.0556 , respectively. **Fig. 3** summarizes the Weibull component k of the HRS and LRS resistances of the PAM and other reported devices, as a function of the standard deviation Δ/μ .¹¹ The Ta/hyperbranched PAM/Pt device exhibits highest k and lowest Δ/μ , which even exceeds the performance of inorganic counterparts. Pulse switching operations were conducted with a write-read-erase-rewrite (WRER) sequence to further study the endurance performance of the PAM devices. The set/reset voltages of the linear and hyperbranched PAMs are $4.0\ \text{V}/-2.0\ \text{V}$ and $3.0\ \text{V}/-2\ \text{V}$, respectively, while the duration of the voltage pulse applied to the Ta/PAM/Pt memory devices is $2\ \mu\text{s}$. The read voltages for both devices are $0.1\ \text{V}$. The memory performance based on these two PAMs is found to be stable for over 5000 WRER cycles (**Fig. S7** of ESI[†]). **Fig. S8** shows the retention capability of the Ta/PAM/Pt memory devices in their LRS and HRS, respectively. The maintenance of the HRS and LRS in the hyperbranched PAM device under $0.1\ \text{V}$ constant voltage stress for $1 \times 10^4\ \text{s}$, suggests that the superior device performance may be obtained by utilizing polymers with hyperbranched structure in thin film devices.

The resistive switching mechanism of the Ta/PAM/Pt memory devices can be attributed to the charge trapping and detrapping in the PAM backbones.¹² As shown in **Scheme 1**, the

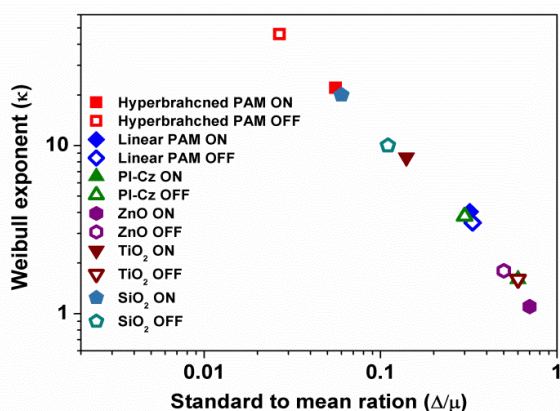


Fig. 3 Weibull exponent (k) versus standard deviation to mean ratio (Δ/μ) for the HRS and LRS resistances of the PAM and other reported devices.

terminal aldehyde groups and nitrogen atoms of the azomethine and triphenylamine chromophores may act as the nucleophilic and electrophilic trapping site, respectively.^{7b,12a} When a positive voltage with sufficient amplitude is applied, the traps will become fully filled with holes. The subsequently injected holes from the electrode can migrate more freely in the polymer thin film, and switch the device from the HRS to the LRS. With the enhanced isotropic architecture in the hyperbranched PAM thin films, charge carrier transport becomes more efficient and stable, which accounts for the superior switching performance in the Ta/PAM/Pt devices.^{11e} When the negative reset voltage is applied to the devices, the filled traps are detrapped to regenerate the potential well for charge carrier hopping, and switch the device back to HRS.^{12a}

In summary, linear and hyperbranched PAMs with identical chemical structure but different molecular geometries and crystalline qualities have been successfully synthesized via condensation polymerization and explored for resistive switching performance. Both polymer exhibit smaller switching voltages of -0.41 V/1.4 V and -0.53 V/1.73 V, ON/OFF ratios over 100, endurance capability for more than 5000 cycles and retention time exceeding 10^4 s. In comparison, the hyperbranched PAM thin film with isotropic architecture demonstrates uniform distribution of the HRS and LRS resistances, which is beneficial for practical memory device applications.

The authors acknowledge the financial supports from the State Key Project of Fundamental Research of China (973 Program, 2012CB933004), National Natural Science Foundation of China (51303194, 11274321, 61328402, 21074034), Ningbo Science and Technology Innovation Team (2011B82004), Ningbo Natural Science Foundations (2013A610031).

Notes and references

^aKey Laboratory of Magnetic Materials and Devices, Zhejiang Province Key Laboratory of Magnetic Materials and Application Technology, Ningbo Institute of Materials Technology and Engineering, Chinese Academy of Sciences, Ningbo, 315201, P. R. China

E-mail: liug@nimte.ac.cn; runwei@nimte.ac.cn

^bDepartment of Physics, Ningbo University, Ningbo 315211, China

^cInstitute of Applied Chemistry, East China University of Science and Technology, Shanghai, 200237, China

E-mail: chentangyu@yahoo.com

[§]These authors contribute equally to this work.

- (a) Emerging research devices. In: International Technology Roadmap for Semiconductors (ITRS) 2005 edn 1–70 (Semiconductor Industry Association, International Sematech, Austin, TX, 2005); (b) Q. D. Ling, D. J. Liaw, C. X. Zhu, D. S. H. Chan, E. T. Kang and K. G. Neoh, *Prog. Polym. Sci.*, 2008, **33**, 917.
- (a) T. C. Chang, F. Y. Jian, S. C. Chen and Y. T. Tsai, *Mater. Today*, 2011, **14**, 608; (b) S. B. Long, C. Cagli, D. Ielmini, M. Liu and J. Sune, *J. Appl. Phys.*, 2012, **111**, 074508; (c) X. J. Zhu, W. J. Su, Y. W. Liu, B. L. Hu, L. Pan, W. Lu, J. D. Zhang and R.-W. Li, *Adv. Mater.*, 2012, **24**, 3941; (d) J. Shang, G. Liu, H. L. Yang, X. J. Zhu, X. X. Chen, H. W. Tan, B. L. Hu, L. Pan, W. H. Xue and R.-W. Li, *Adv. Funct. Mater.*, 2014, **24**, 2171.
- (a) G. Liu, B. Zhang, Y. Chen, C. X. Zhu, L. J. Zeng, D. S. H. Chan, K. G. Neoh, J. N. Chen and E. T. Kang, *J. Mater. Chem.*, 2011, **21**, 6027; (b) K. L. Wang, Y. L. Liu, J. W. Lee, K. G. Neoh and E. T. Kang, *Macromolecules*, 2010, **43**, 7159; (c) H. C. Wu, A. D. Yu, W. Y. Lee, C. L. Liu and W. C. Chen, *Chem. Commun.*, 2012, **48**, 9135; (d) D. J. Liaw, K. L. Wang, Y. C. Huang, K. R. Lee, J. Y. Lai and C. S. Ha, *Prog. Polym. Sci.*, 2012, **37**, 907; (e) J. H. Wu, H. J. Yen, Y. C. Hu and G. S. Liou, *Chem. Commun.*, 2014, **50**, 4915.
- (a) J. M. J. Fréchet, *Science*, 1994, **263**, 1710; (b) X. T. Tao, Y. D. Zhang, T. Wada, H. Sasabe, H. Suzuki, T. Watanabe, S. Miyata, *Adv. Mater.*, 1998, **10**, 226; (c) X. M. Liu, C. B. He, X. T. Hao, L. W. Tan, Y. Q. Li, K. S. Ong, *Macromolecules*, 2004, **37**, 5965.
- (a) H. Siringhaus, P. J. Brown, R. H. Friend, M. M. Nielsen, K. Bechgaard, B. M. W. Langeveld-Voss, A. J. H. Spiering, R. A. J. Janssen, E. W. Meijer, P. Herwig, et al., *Nature*, 1999, **401**, 685; (b) H. Yang, T. J. Shin, L. Yang, K. Cho, C. Y. Ryu, Z. Bao, *Adv. Funct. Mater.*, 2005, **15**, 671; (c) J. Roncali, P. Leriche, A. Cravino, *Adv. Mater.*, 2007, **19**, 2045.
- (a) L. Pan, B. L. Hu, X. J. Zhu, X. X. Chen, J. Shang, H. W. Tan, H. Xue, Y. J. Zhu, G. Liu and R.-W. Li, *J. Mater. Chem. C*, 2013, **1**, 4556; (b) B. L. Hu, X. J. Zhu, X. X. Chen, L. Pan, S. S. Peng, Y. Z. Wu, J. Shang, G. Liu, Q. Yan and R.-W. Li, *J. Am. Chem. Soc.*, 2012, **134**, 17408; (c) M. A. Khalid, A. G. El-Shekeil and F. A. Al-Yusufy, *Eur. Polym. J.*, 2001, **37**, 1423; (d) L. Song, C. L. Tu, Y. F. Shi, F. Qiu, L. He, Y. Jiang, Q. Zhu, B. S. Zhu, D. Y. Yan and X. Y. Zhu, *Macromol. Rapid Commun.*, 2010, **31**, 443.
- (a) H. J. Niu, P. H. Luo, M. L. Zhang, L. Zhang, L. N. Hao, J. Luo, X. D. Bai and W. Wang, *Eur. Polym. J.*, 2009, **45**, 3058; (b) H. J. Niu, Y. D. Huang, Y. D. Bai, X. Li and G. L. Zhang, *Mater. Chem. Phys.*, 2004, **86**, 33.
- (a) F. Ania, F. J. Balta-Calleja, A. Flores, G. H. Michler, S. Scholtyssek, D. Khariwala, A. Hiltner, E. Baer, L. Rong and B. S. Hsiao, *Eur. Polym. J.*, 2012, **48**, 86; (b) G. Shen, V. A. Piunova, S. Nutt and T. E. Hogen-Esch, *Polymer*, 2013, **54**, 5790.
- (a) J. N. L. Albert, W. S. Young, R. L. Lewis, T. D. Bogart, J. R. Smith and T. H. Epps, *ACS Nano*, 2012, **6**, 459; (b) J. A. Yoon, T. Young, K. Matyjaszewski and T. Kowalewski, *ACS Appl. Mater. Interfaces*, 2010, **2**, 2475; (c) C. J. Lu, Q. Liu, P. Y. Gu, D. Y. Chen, F. Zhou, H. Li, Q. F. Xu and J. M. Lu, *Polym. Chem.*, 2014, **5**, 2602.
- (a) W. Weibull, *J. Appl. Mech.*, 1951, **18**, 293; (b) S. B. Long, X. J. Lian, C. Cagli, L. Perniola, E. Miranda, M. Liu and J. Sune, *IEEE Electron Device Lett.*, 2013, **34**, 999.
- (a) B. J. Choi, A. B. K. Chen, X. Yang and I. W. Chen, *Adv. Mater.*, 2011, **23**, 3847; (b) W. Y. Chang, K. J. Cheng, J. M. Tsai, H. J. Chen, F. Chen, M. J. Tsai and T. B. Wu, *Appl. Phys. Lett.*, 2009, **95**, 3; (c) B. L. Hu, F. Zhuge, X. J. Zhu, S. S. Peng, X. X. Chen, L. Pan, Q. Yan and R. W. Li, *J. Mater. Chem.*, 2012, **22**, 520; (d) Y. C. Yang, F. Pan, Q. Liu, M. Liu and F. Zeng, *Nano Lett.*, 2009, **9**, 1636; (e) D. C. Kim, M. J. Lee, S. E. Ahn, S. Seo, J. C. Park, I. K. Yoo, I. G. Baek, H. J. Kim, E. K. Yim, J. E. Lee, S. O. Park, H. S. Kim, U. I. Chung, J. T. Moon and B. I. Ryu, *Appl. Phys. Lett.*, 2006, **88**, 3.
- (a) S. H. Hong, O. Kim, S. Choi and M. Ree, *Appl. Phys. Lett.*, 2007, **91**, 3; (b) J. Y. Ouyang, *Appl. Phys. Lett.*, 2013, **103**, 4; (c) R. T. Weitz, A. Walter, R. Engl, R. Sezi and C. Dehm, *Nano Lett.*, 2006, **6**, 2810; (d) R. J. Tseng, J. X. Huang, J. Ouyang, R. B. Kaner and Y. Yang, *Nano Lett.*, 2005, **5**, 1077.